ECE 445

SENIOR DESIGN LABORATORY

DESIGN DOCUMENT

Sensing your heartbeat (and others)

Team #32

XIN CHEN
(xin13@illinois.edu)
YUKAI HAN
(yukaih3@illinois.edu)
XUANQI WANG
(xuanqiw3@illinois.edu)
QIYANG WU
(qiyangw2@illinois.edu)

Sponsor: Howard Yang

April 13, 2025

Contents

1 Introduction

1.1 Problem & Solution Overview

1.1.1 Problem Description

With fertility rates falling and young people under increasing pressure to work, more and more older people are now living at home alone. In other words, many elderly people are currently in a state of unattended care at home, and if they faint at home in a sudden illness, the consequences are incalculable. Therefore, a big challenge of the elderly care problem today is how to accurately monitor the health of the elderly in the home environment and timely feedback when problems occur and then take appropriate measures. Nowadays, most monitoring systems rely on specialized hardware like wearable sensors or cameras. These subjects, however, could be costly and inconvenient for older people to use. In that case, WiFi signal, as a ubiquitous object around our lives, is a good choice to provide non-contact sensing which cannot be achieved by traditional monitoring systems. Despite the convenience that WiFi signals convey, it is still a problem that extracting and interpreting Channel State Information (CSI) accurately and making use of them to detect subtle human activities such as breathing and heartbeats with the interference from the outside environment.

To be specific, two main problems appear in the traditional systems. One is unavoidable physical contact like the chest straps it contains. Although the existing medical technology has minimized the discomfort caused by such contact, they are unsuitable for some certain applications and people. Another issue that conventional methods have is the cost and limited accessibility. Some wearable health monitoring devices are often expensive and even if they can afford it. Taking a burden on the body always affects and restricts their normal activities. Then for WiFi-based sensing method, the major problem is concentrated on the environmental interference. The signal might be influenced by noise and dynamic surroundings easily, making it hard to extract exact physiological signals.

1.1.2 Solution

Respiratory diseases are one of the biggest threats to the health of the elderly. Real-time acquisition of human respiratory information is extremely important for health management and risk warning and helps to diagnose respiratory diseases. The aim is to achieve accurate, real-time, non-contact monitoring of human respiratory conditions in the home environment and provide convenience for health management and old-age care.

The approach will extract fine-grained CSI data from a WiFi transmitter-receiver setup. The signal will reflect subtle physiological activities like breathing and heartbeats. By analyzing the amplitude and phase variations of signals when they interact with the human body, we can infer the breath or heartbeat rates. To make it visually intuitive, we will map the data to some LED indicators lying on a chest model and these lights could flash in sync with the measured activities frequency. Moreover, we add a ground truth measurement system to make comparison. This system will use a respiration or heartbeat belt to provide accurate physiological data for validation with another group of LED in-

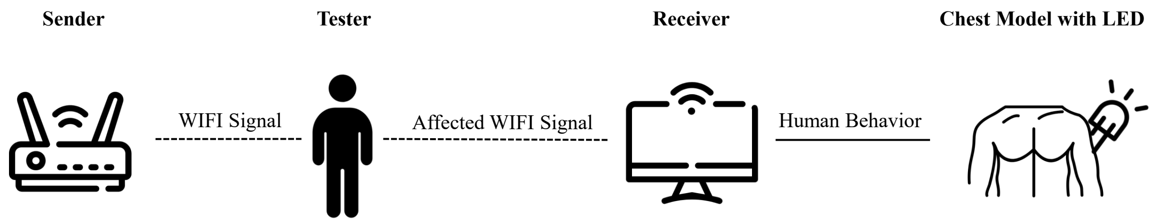

Figure 1: Visual aid

dicators.

To implement our system, a WiFi sensing network is needed. We will equip this network with AX200 cards for both transmitter and receiver to achieve CSI extraction. During the experiment process, the receiver will take the CSI data by Ubuntu 22.04 LTS and PicoScenes software and then apply filtering and signal processing algorithms to reduce environmental noise. The processed activity frequency will then be used to modulate LED flashing frequency, making the experiment visually. In addition, a ground truth which is behaved as a control group will exist and it will use the belt data to ensure reliability.

1.2 Visual aid

The whole process without ground truth is shown in Figure 1. A WiFi transmitter (Sender) will emit signals and then these signals will be affected by tester's movements before being accepted by a WiFi receiver (Receiver). The receiver will then process the CSI to analyze tester's behavior patterns. Finally this extracted data will be mapped onto a chest model with some LED indicators, making the behavior rate visually.

1.3 High-level requirements list

- The system should accurately detect human behavior patterns using WiFi CSI data, with a minimum correlation of **70%** compared to the behavior ground truth measurements.
- The system must be able to visualize behavior data in real-time with a maximum delay of **750 milliseconds** between data acquisition and LED output to ensure immediate feedback for health monitoring
- The system must maintain consistent behavior detection with sufficient environmental noise such as background movement and multipath effects and give an accuracy that does not drop below **70%** in different indoor conditions.

2 Design

2.1 Block Diagram

See Figure 2

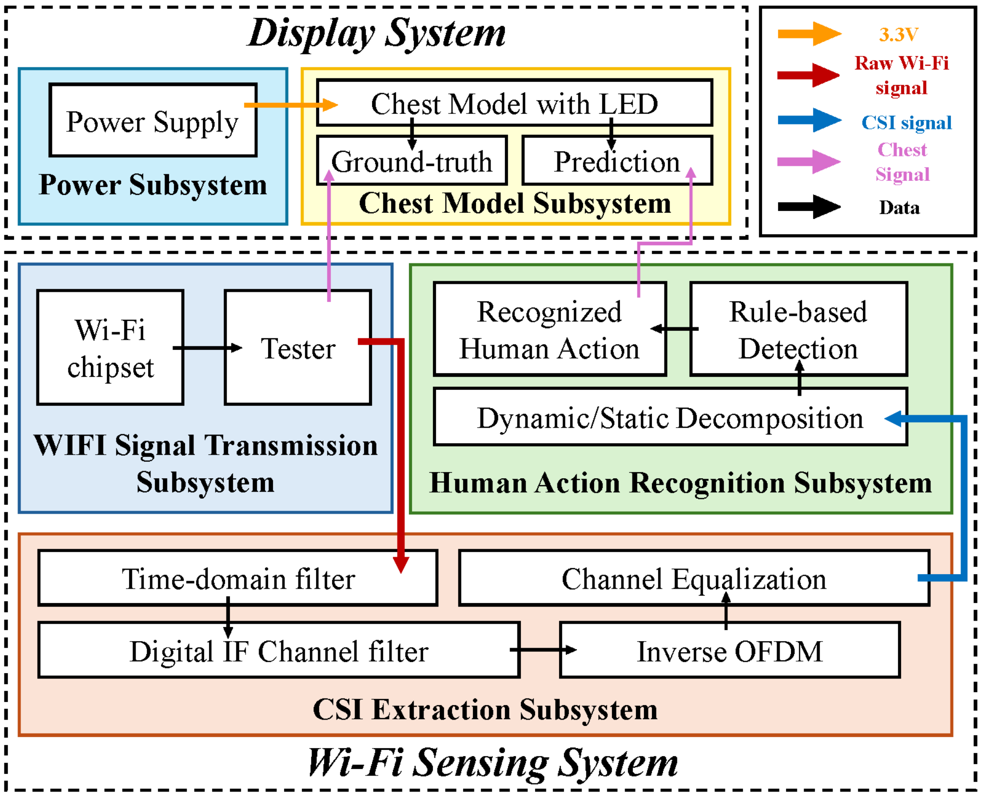

Figure 2: Block Diagram

2.2 Physical Design

The physical design of our team is shown in Figure 3. The main components are the sender and receiver connected with WiFi signal amplifiers. PCB board used to transmit the CSI signal. At the same time, two chest models are placed in the surroundings, with LED lights and counters to visualize the results. The figure does not depict the specific experimental device of ground truth, which needs to tie a belt to the tester's body and then plug the USB flash drive into the Receiver to output the image.

As shown in the figure, the receiver is connected to the PCB to transmit the WiFi signal and the ground truth output. The PCB board processes the signal and controls the flashing of LED lights and the number in counters. We wanted to reflect the tester's breathing rate through the blinking of the LED lights and display the real-time breathing rate through the counter. Moreover, the ideal test environment in our imagination is to ensure that there are not too many people close to the tester to avoid affecting the test result. In addition, the distance between the tester and the test table should be kept at 2-5cm. During the test, avoid large movements and loud speech, and maintain natural breathing under normal conditions. The test results could then be more accurate.

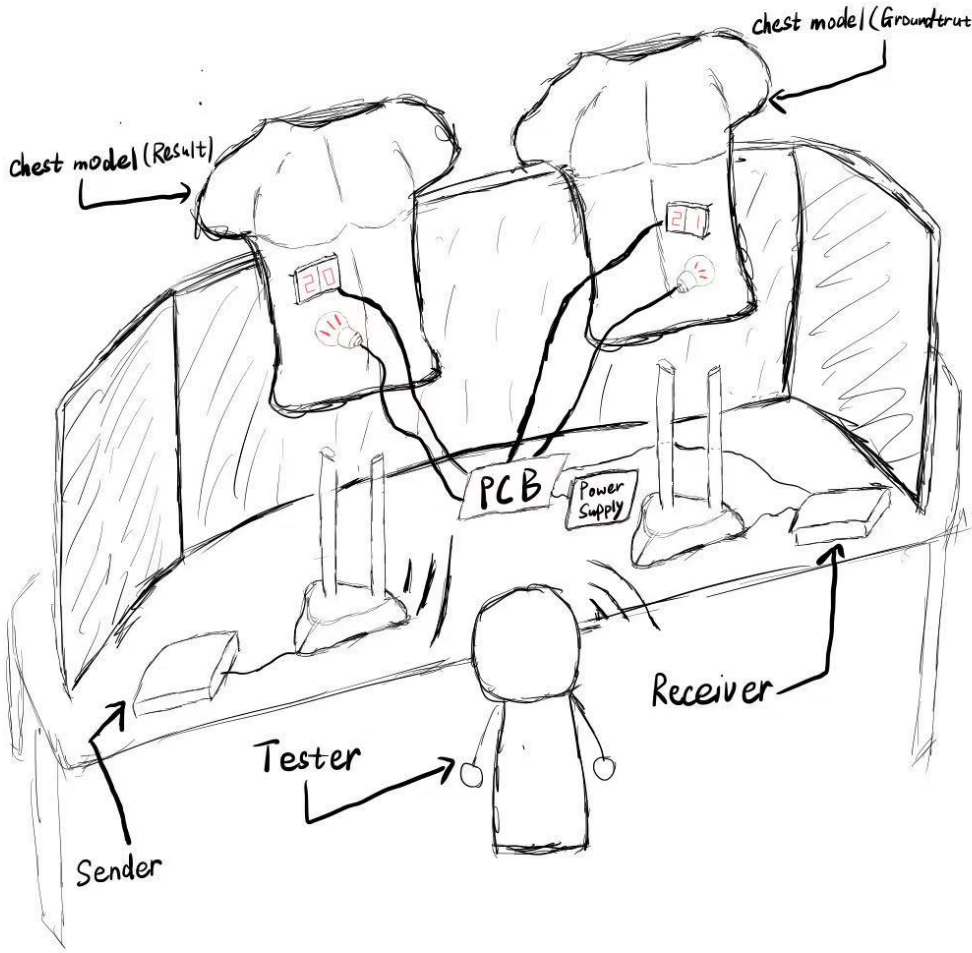

Figure 3: Physical Design

2.3 WiFi Sensing System

2.3.1 WiFi Signal Transmission Subsystem

The WiFi Signal Transmission Subsystem forms the foundation of the entire wireless sensing infrastructure, establishing a stable and high-fidelity communication channel that is essential for accurate signal acquisition and processing. To support flexible deployment in diverse indoor environments, the system is designed to operate in both 2.4GHz and 5GHz dual bands, offering resilience against interference and improving overall signal quality. In order to guarantee the accuracy of channel state information (CSI) acquisition, the subsystem must maintain a minimum signal-to-noise ratio (SNR) of 20dB, ensuring that minor environmental perturbations—such as those caused by human motion or breathing—can be captured reliably.

Moreover, real-time performance is a critical requirement for this subsystem, especially in latency-sensitive applications like respiratory monitoring. As such, the end-to-end signal transmission latency is constrained to be under 100 milliseconds, enabling the rapid delivery of CSI data to downstream processing units.

To safeguard data integrity, it is imperative that the operating environment remains free from extraneous wireless interference, which could distort the raw Wi-Fi signals or introduce unwanted noise into the CSI. This includes minimizing the presence of active devices on the same channel and controlling the electromagnetic environment.

Equally important is the subject control during measurements. To ensure that the extracted CSI patterns are solely attributed to the target individual's micro-movements (e.g., chest displacement due to breathing), the environment should have less interference. This restriction is vital for reducing cross-subject interference and ensuring that the resulting data reflects a clean, interpretable signal profile corresponding to a single individual's actions.

Together, these stringent requirements enable the WiFi Signal Transmission Subsystem to provide high-precision, low-latency, and interference-resilient CSI streams—laying the foundation for subsequent modules in the Wi-Fi sensing system to perform accurate signal decomposition and human activity recognition.

Table 1: R&V for WiFi Signal Transmission Subsystem

Requirement	**Verification**
• Signal-to-noise ratio (SNR) of at least 20 dB must be maintained at the receiver under nominal operating conditions. • End-to-end signal transmission latency must not exceed 100 ms.	• Measure SNR in a low-interference environment using network diagnostic tools (e.g., Wireshark with CSI tool or custom SNR monitoring scripts); confirm SNR $>$ 20 dB. • Use a network analyzer or embedded software timestamps to measure transmission delay; ensure latency $<$ 100 ms.

2.3.2 CSI Extraction Subsystem

The CSI Extraction Subsystem is a critical component responsible for accurately translating raw WiFi signals into precise CSI data necessary for further analysis. To achieve this, the subsystem incorporates several sophisticated signal processing modules, including Time Domain Filtering, Digital IF Channel Filtering, Inverse OFDM transformation, and Channel Equalization.

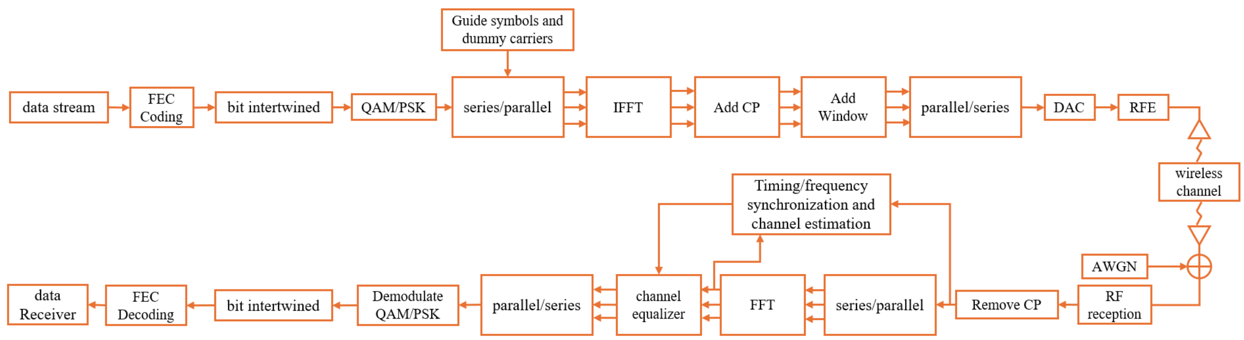

Figure 4: CSI Extraction Process

Time Domain Filter

The first processing stage involves a time domain filter, which significantly enhances signal integrity by suppressing temporal noise and interference. This filter operates by selectively attenuating frequencies outside the desired band, thus preserving signal components essential for accurate CSI extraction. Implementing such filters helps maintain consistency in the extracted CSI, particularly under varying environmental conditions, leading to robust and stable data acquisition for downstream processing.

Digital IF Channel Filter

Following time domain filtering, the digital Intermediate Frequency (IF) channel filter further refines signal quality. It operates digitally to isolate the intermediate frequencies required for channel state information extraction. The filter removes residual out-of-band noise and interference that could distort the CSI measurements. Digital IF filtering ensures a high signal-to-noise ratio (SNR), critical for maintaining the precision of CSI data in high-density signal environments.

Inverse OFDM

Orthogonal Frequency Division Multiplexing (OFDM) is fundamental to WiFi systems due to its resilience against multipath fading. In the CSI Extraction Subsystem, Inverse OFDM (IOFDM) plays a pivotal role. This module converts frequency-domain data received from WiFi transmissions back to the time domain. This transformation is essential as it facilitates detailed channel characterization by converting CSI data into a form suitable for precise temporal analysis, thereby enabling accurate detection of subtle variations caused by human movements.

Channel Equalization

Channel equalization is the final yet crucial step in the CSI extraction process. Due to multipath propagation and various hardware imperfections such as IQ imbalance, signals undergo amplitude and phase distortions. Channel equalization corrects these distortions, aligning the received signal closer to the original transmitted state. Techniques such as Minimum Mean Square Error (MMSE) equalization are employed to minimize error, enhancing the accuracy and reliability of the extracted CSI.

The MMSE equalizer coefficients are calculated as follows:

$$W_{\text{MMSE}} = (H^H H + \sigma_n^2 I)^{-1} H^H \tag{1}$$

Where:

- W_{MMSE} is the weight matrix for the MMSE equalizer.
- H represents the channel matrix, describing amplitude and phase distortions introduced by the wireless channel.
- H^H denotes the Hermitian transpose (conjugate transpose) of matrix H.
- σ_n^2 is the noise power.
- I is the identity matrix with the same dimensions as $H^H H$.

Equalization ensures the fidelity of CSI data, which directly influences the subsystem's ability to perform sensitive human action recognition and environmental sensing tasks.

Through the seamless integration of these advanced signal processing techniques, the CSI Extraction Subsystem reliably delivers high-quality channel state information, thus underpinning the effectiveness of the entire WiFi sensing system.

Table 2: R&V for CSI Extraction Subsystem

Requirement	**Verification**
• The end-to-end processing delay of the CSI extraction process from receiving the WiFi signal to outputting the CSI data shall not exceed 60 ms. • The system should have a certain anti-interference ability, can be in the ordinary WiFi frequency band under the environment of stable extraction of CSI information.	• Use a high-precision timer to record, averaged over at least 300 independent measurements to see if the average processing delay is less than 60 ms. • Run the system in a typical indoor WiFi environment for more than 10 minutes and verify that data volatility is within acceptable thresholds.

2.3.3 Human Action Recognition Subsystem

The Human Action Recognition Subsystem is designed to transform raw CSI data into clear and meaningful features that reveal subtle human actions such as respiration. The system's input, continuously captured CSI measurements, is first managed using a circular buffering mechanism that ensures low-latency storage of the most recent data. This guarantees that the processing pipeline always operates on up-to-date CSI signals while keeping the memory usage under control. Next, the subsystem computes the ratio between CSI readings obtained from two antennas. This operation effectively cancels out static multipath effects and common-mode noise, isolating the dynamic component that corresponds to small-scale movements of the human body. Given the intrinsic challenges in commercial WiFi systems—such as abrupt phase jumps caused by hardware-induced phase ambiguity—the subsystem employs a dedicated phase correction step. This step uses a histogram-based method and complex rectification to resolve the two-way (binary) phase ambiguity, thus restoring the continuity of the phase information. Finally, a Savitzky–Golay filter is applied to the CSI ratio waveform to attenuate high-frequency noise while preserving the low-frequency, periodic characteristics inherent to respiratory movements. As a result, the output of the Human Action Recognition Subsystem can be either a clean, smoothed waveform that faithfully represents the underlying human signal or an estimation of the periodic frequency of the action (e.g., the respiration rate). This end-to-end process enables reliable detection and monitoring of human physiological activities based solely on the analysis of commodity WiFi CSI data.

Step1: Circular Buffering Real-time CSI Data

In this initial step, the system employs a circular buffering mechanism to manage real-time CSI data with low latency. The primary goal of using a circular buffer is to ensure that the CSI management process remains both efficient and responsive. A fixed-length buffer is continuously updated with the most recent CSI measurements, and once it reaches capacity, newly received data immediately overwrite the oldest entries. This design choice is critical for achieving low-latency processing, as it eliminates the need for time-consuming memory reallocation or data shifting operations, thereby enabling rapid access to fresh data.

The circular buffer not only provides an efficient way to store continuously incoming CSI measurements but also maintains a stable time-window that captures the signal's temporal dynamics. This persistent update facilitates the detection of subtle low-frequency variations. By consistently working with the most current set of CSI data, the system can promptly capture transient events and changes in the wireless channel, ensuring that processing modules downstream can operate on the latest information without delay.

Furthermore, the circular buffering approach optimizes memory usage by constraining the stored dataset to a predetermined size. This controlled memory footprint prevents excessive resource consumption while still delivering the necessary temporal context for accurate feature extraction. In sum, the circular buffering mechanism is designed to underpin real-time, low-latency CSI data management. It strikes a balance between ensuring a timely response to signal changes and maintaining data continuity, ultimately laying a robust foundation for subsequent steps in processing.

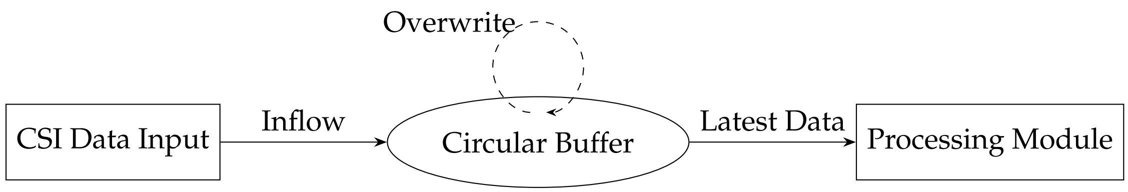

Step2: Obtaining Dynamic Component by CSI Ratio

In this step, the system exploits the ratio of CSI readings from two antennas to isolate the dynamic component induced by subtle human motion (e.g., respiration) while suppressing the static multipath effects from the environment, as proposed by [1]. Let $H_1(f,t)$ and $H_2(f,t)$ denote the complex CSI measurements from two antennas at frequency f and time t. These measurements can be modeled as

$$H_i(f,t) = e^{-j\theta_{\text{offset}}}\Big[H_{s,i}(f,t) + A_i(f,t)e^{-j\frac{2\pi d_i(t)}{\lambda}}\Big], \quad i = 1, 2,$$

where $H_{s,i}(f,t)$ represents the static multipath components, $A_i(f,t)$ is the amplitude of the dynamic (motion-induced) component, $d_i(t)$ is the time-varying path length affected by body movement, λ is the wavelength, and $e^{-j\theta_{\text{offset}}}$ is the common phase offset caused by unsynchronized hardware.

Since both antennas share the same radio frequency oscillator, the phase offset cancels out when the ratio is taken:

$$R(f,t) = \frac{H_1(f,t)}{H_2(f,t)} = \frac{H_{s,1}(f,t) + A_1(f,t)e^{-j\frac{2\pi d_1(t)}{\lambda}}}{H_{s,2}(f,t) + A_2(f,t)e^{-j\frac{2\pi d_2(t)}{\lambda}}}.$$

Assuming that the difference between the dynamic path lengths is approximately constant,

$$d_2(t) \approx d_1(t) + \Delta d,$$

the above expression can be rewritten as

$$R(f,t) = \frac{H_{s,1}(f,t) + A_1(f,t)e^{-j\frac{2\pi d_1(t)}{\lambda}}}{H_{s,2}(f,t) + A_2(f,t)e^{-j\frac{2\pi \Delta d}{\lambda}}e^{-j\frac{2\pi d_1(t)}{\lambda}}}.$$

By dividing the numerator and the denominator by $e^{-j\frac{2\pi d_1(t)}{\lambda}}$, we obtain

$$R(f,t) = \frac{A_1(f,t) + H_{s,1}(f,t)e^{j\frac{2\pi d_1(t)}{\lambda}}}{A_2(f,t)e^{-j\frac{2\pi \Delta d}{\lambda}} + H_{s,2}(f,t)e^{j\frac{2\pi d_1(t)}{\lambda}}}.$$

This formulation effectively cancels common factors—such as the random phase offset and shared static multipath effects—thereby accentuating the small variations in $d_1(t)$ due to human motion. As a result, the CSI ratio $R(f,t)$ primarily reflects the dynamic changes (e.g., the minute chest movements during breathing) and generally appears as a circular

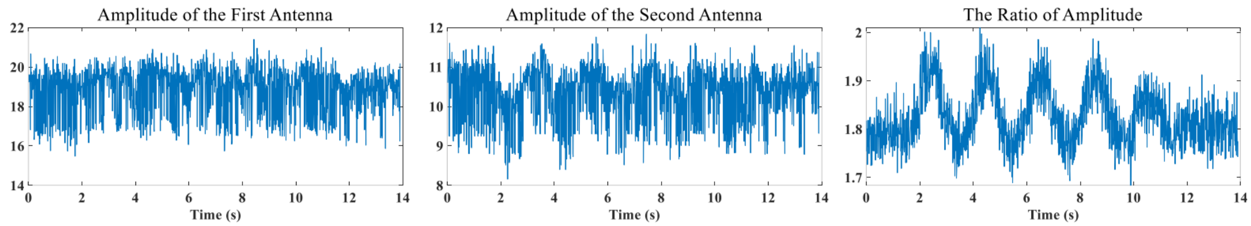

Figure 5: Comparison of three amplitude waveforms when a subject moves further away. Obviously, the ratio of amplitude outperforms the other two raw amplitude waveforms for its clear fluctuation caused by the movements.

or arc-like trajectory in the complex plane when the displacement is small (typically a fraction of the wavelength).

In summary, by taking the ratio of two CSI measurements, the system eliminates common-mode noise and enhances sensitivity to the dynamic component. The amplitude of the ratio represents the relative strength of the signals, while its phase encodes the subtle motion-induced changes. This makes the CSI ratio a robust metric for capturing and processing the dynamic variations associated with human respiration.

Step3: Phase Correction

As noted in [2], [3], commercial WiFi devices suffer from inherent hardware impairments that lead to abrupt phase jumps in the measured CSI data. In particular, cards such as the Intel AX200 typically exhibit a binary phase ambiguity. This phenomenon arises largely due to the behavior of the phase-locked loop (PLL) in the receiver chain. Specifically, the PLL tends to lock onto the nearest 180° phase, leading the measured phase $\hat{\theta}$ to adopt one of two values:

$$\hat{\theta} = \theta + k\pi, \quad k \in \{0, 1\},$$

where θ represents the true phase and $k = 1$ indicates an undesired phase jump by π. Such discontinuities distort the trajectory of the CSI ratio in the complex plane, making it difficult to discern the subtle phase variations caused by human motions.

To mitigate this ambiguity, the method exploited in our project utilizes a histogram-based and complex rectification approach [4]. Over a short time window, the measured phase differences are aggregated into a histogram. Typically, the histogram reveals a bimodal distribution with two dominant peaks corresponding to θ and $\theta + \pi$. By identifying the valley between these two peaks, a decision boundary θ_v is determined. Then, each CSI sample represented by its complex value $z = Ae^{j\hat{\theta}}$ is corrected by applying a simple mapping:

$$\tilde{z} = \begin{cases} z, & \text{if } \hat{\theta} \le \theta_v, \\ -z, & \text{if } \hat{\theta} > \theta_v. \end{cases}$$

This operation effectively "flips" the samples where a π jump has occurred, thereby restoring the continuity of the phase. The corrected phase $\tilde{\theta}$ then reflects a smoother variation over time, which is essential for capturing the low-amplitude human motion signal.

Furthermore, when the corrected CSI data are plotted in the complex plane, they are expected to form a continuous circular arc. Any residual discontinuities due to phase ambiguity would interrupt this arc, but the combination of histogram division and complex rectification ensures the recovered phase dynamics are consistent with the expected behavior of the dynamic component. Overall, this phase correction step is crucial for eliminating the distortions caused by the hardware-induced phase jumps and for enabling reliable extraction of the subtle motion-induced signal variations.

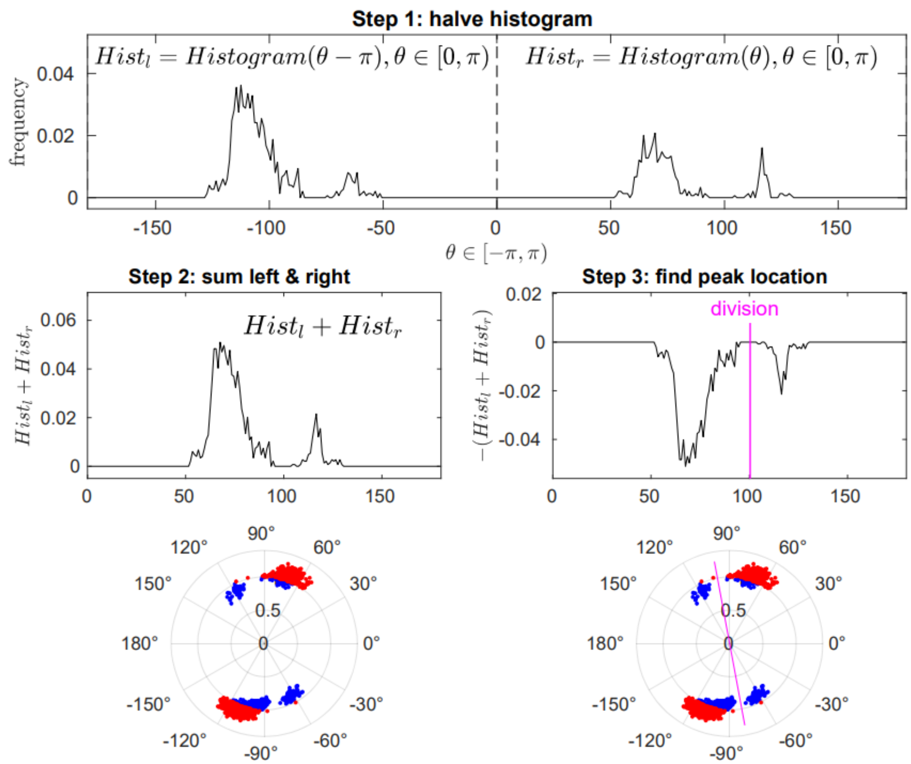

Figure 6: The process of finding the division boundary through histogram dividing and complex rectifying method, from [4]

Step4: Filter Smoothing

To suppress high-frequency noise and to robustly extract the subtle human motion signal embedded in the CSI ratio, the system employs a Savitzky–Golay (S-G) filter. The S-G filter is a polynomial smoothing technique that works by fitting a low-degree polynomial to successive segments of the data using linear least squares. For each data point, the filter computes a weighted average of its neighbors, where the weights are derived from the fitted polynomial, thereby preserving important features (such as peak height and waveform shape) better than simple moving average filters.

Mathematically, suppose the original signal is represented by a set of equally spaced points y_i. The S-G filter calculates the smoothed value $\hat{y}_i$ by convolving the original signal with a set of coefficients c_k:

$$\hat{y}_i = \sum_{k=-m}^{m} c_k \, y_{i+k},$$

where $2m + 1$ is the size of the sliding window and the coefficients c_k are computed by fitting a polynomial $P(t)$ of degree p to the data points in the window:

$$P(t) = a_0 + a_1 t + a_2 t^2 + \cdots + a_p t^p.$$

The coefficients are chosen such that the squared error between the polynomial and the actual data over the window is minimized. In effect, the filtering operation can be seen as a convolution, where the filter's impulse response is calculated from the solution of the linear least-squares problem.

One of the key advantages of the S-G filter is its ability to preserve the essential shape characteristics of the waveform—such as the amplitude and relative locations of peaks and valleys—while effectively reducing high-frequency fluctuations. This property is especially critical in our application because the respiratory-induced variations in the CSI ratio are often of very low amplitude and can be easily masked by noise. By preserving these subtle characteristics, the filter ensures that subsequent possible steps, like peak detection and motion rate estimation, can operate on a signal that accurately reflects the true physiological motion.

Table 3: R&V for Human Action Recognition Subsystem

Requirement	**Verification**
• Real-time: Process CSI with latency < 100 ms. • Accuracy: Respiration error $<$ 0.2 bpm.	• Measure total latency to confirm < 100 ms. • Lab tests with a reference wearable device.

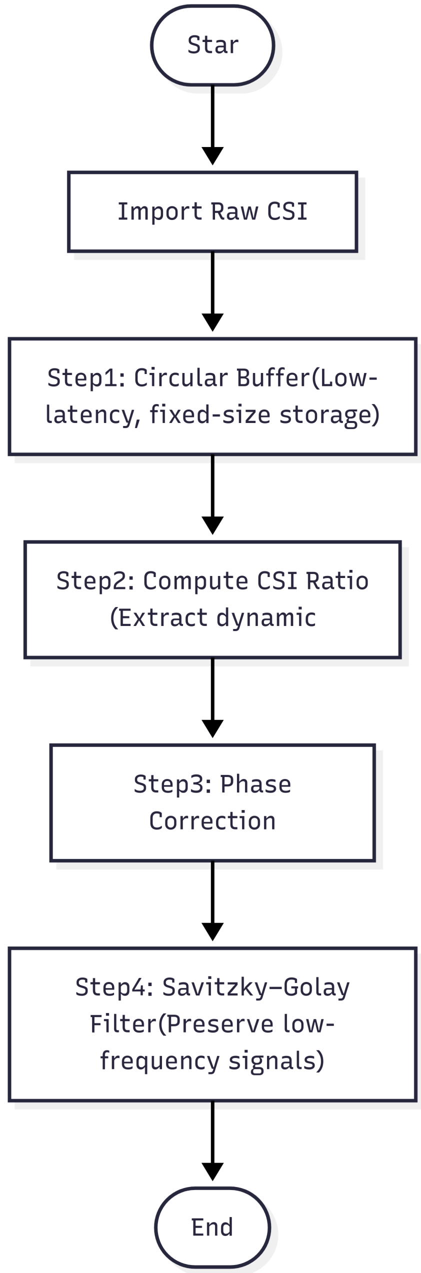

Figure 7: Flowchart of Human Action Recognition Subsystem

2.4 Display System

2.4.1 Power Subsystem

The Power Subsystem is tasked with delivering stable and efficient electrical energy to the entire display system, with a specific emphasis on ensuring reliable power for both the chest model's LED array and the PCB control circuitry. Since LEDs are highly sensitive to variations in both voltage and current, it is critical that the system provides a consistently stable 3.3 V DC output with a tolerance of only ±10% to ensure uniform brightness and consistent performance. To accommodate the substantial inrush and transient surge currents typically seen at LED startup, the power module must be capable of delivering a minimum current of 500mA for the LED array.

In parallel, the PCB controller requires a dedicated 12 V power input. Maintaining a clean and stable 12 V supply is essential to ensure the correct operation of the digital logic, signal processing, and interfacing components housed on the PCB. The dual-voltage requirement necessitates either separate regulated outputs or an onboard DC-DC conversion scheme to efficiently provide both voltage rails from a common input source.

The power system implements a switching power supply architecture as shown in figure 8 to generate the 3.3 V voltage for the LED array and 12 V for the PCB controller. This configuration involves a PWM-controlled switching component paired with essential inductors, rectification diodes, and filtering capacitors to effectively reduce the input voltage. A high-efficiency feedback mechanism continuously monitors the output voltage and dynamically adjusts the PWM duty cycle to rapidly respond to changes in load conditions, ensuring stability across operating modes. Additionally, overcurrent and short-circuit protection circuits are integrated into both voltage supply paths, allowing the system to quickly detect abnormal current surges and either limit or shut off the output to prevent damage. These protections safeguard not only the LED array but also the PCB from the risks posed by unexpected short circuits or excessive transient loading.

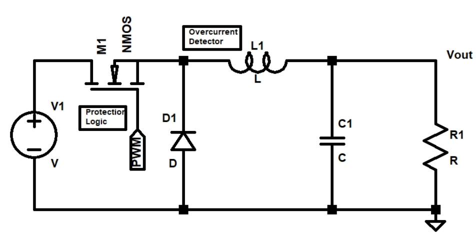

Figure 8: The Circuit Schematic of the Power Subsystem

Efficiency is a paramount consideration for this power subsystem. The design targets a conversion efficiency of at least 75%. High efficiency reduces energy loss, minimizes thermal buildup, and simplifies thermal management requirements. Given that experimental and demonstration scenarios may require the system to operate continuously for 1 hour or more, it is essential that the power subsystem delivers long-duration reliability under varying load conditions.

In summary, a power subsystem that satisfies stringent requirements for voltage stability, current capability, and conversion efficiency is foundational to the system's performance and reliability. By combining high-efficiency switching techniques with robust protection mechanisms, the design ensures uninterrupted and safe operation of both the LED lighting and PCB control systems.

Table 4: R&V for Power Subsystem

Requirement	**Verification**
• The power subsystem must provide a stable 3.3 V DC output with a tolerance of ±10% under a load of up to 500 mA for the LED array • It must provide a stable 12 V DC output with a tolerance of ±10% for the PCB controller • The system must support continuous operation for a minimum duration of 1 hour without performance degradation.	• Use a digital multimeter (DMM) or oscilloscope to measure the 3.3 V and 12 V output voltages under nominal load conditions; confirm that the voltages remain within ±10% tolerance • Connect a variable electronic load to simulate the 500 mA (LED) load; observe output stability over time. • Run the system for at least 1 continuous hour and periodically log output voltage, current, and system temperature; check for voltage drift or shutdowns.

2.4.2 Chest Model Subsystem

The Chest Model Subsystem visually represents human action through an LED array installed on a chest cavity model, providing a tangible demonstration of both ground-truth (i.e., the tester's actual actions) and predicted (i.e., the monitored system's recognized) signals for real-time validation of the Human Action Recognition Subsystem. The LED array is arranged to simulate human action, with each LED individually addressable to control brightness based on the strength of the detected signals. This design enables direct comparison between the monitored signal intensity and the actual measured activity. The system must update the LED brightness levels within 50 ms for timely synchronization, and the LEDs should be sufficiently bright for clear observation under typical indoor and outdoor lighting conditions.

A key component enabling this visualization is the PCB controller, which bridges the processed breath signal and LED array on the chest model. After receiving the processed breathing signal, the PCB generates PWM signals to drive the LED array, causing its brightness to vary in sync with the breathing cycle.

Regarding the specific chest model, we originally intended to use 3D printing technology to make the model as shown in Figure 9, but later considered that the quality of the model would be too large, which is not very easy to carry and use. Finally, we decided to use a plastic chest model, and to control its height and width within 40 cm to avoid excessive volume.

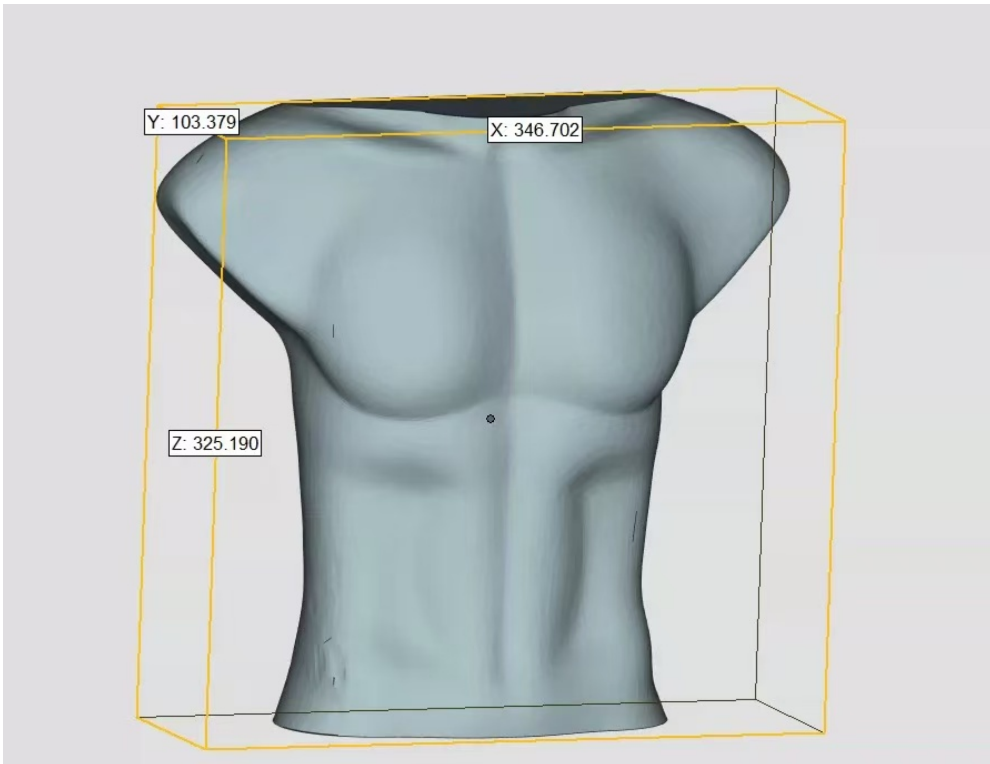

Figure 9: Chest Model

Table 5: R&V for Chest Model Subsystem

Requirement	Verification
• The two chest models are firmly fixed and less than 4kg for easy carrying • The LED array should visibly brighten and dim in sync with user breathing under normal indoor conditions	• Ensure the model is securely fixed on the acrylic base and weighs less than 4 kg using a scale if needed • Have a tester breathe normally and observe whether the LED brightness visibly follows the breathing rhythm

2.5 Tolerance Analysis

A major risk in the design is whether Wi-Fi CSI can reliably detect subtle human behaviors—such as the small chest displacements during breathing—given the inherent noise and multipath interference in indoor environments. Based on Fresnel zone theory[5], our analysis shows that detection sensitivity strongly depends on the subject's position within the Fresnel zones.

For example, at a Wi-Fi frequency of 5.24GHz, the wavelength λ is approximately 57mm. A typical chest displacement during normal breathing is about 5mm. According to the Fresnel zone model, the phase change $\Delta\phi$ induced by this displacement is given by:

$$\Delta\phi = \frac{2\pi\,\Delta d}{\lambda}, \tag{2}$$

where Δd is the displacement. Substituting the values:

$$\Delta\phi \approx \frac{2\pi \times 5mm}{57mm} \approx 0.55 \text{ radians} \quad (\approx 31.6^\circ). \tag{3}$$

This phase shift, although small, is within detectable limits provided that the system's phase resolution is on the order of 0.1 radians. However, this detection is critically sensitive to the target's location:

- **Optimal Detection:** When the subject is centered within a Fresnel zone, the interference between the direct and reflected signals yields maximum phase sensitivity.
- **Degraded Detection:** When the subject is near the Fresnel zone boundaries, the phase contributions may partially cancel out, reducing the effective signal change and making detection more vulnerable to noise.

The analysis shows that, under controlled conditions with stable noise levels (phase noise less than 0.1 radians RMS), a phase shift of 0.55 radians is discernible. This confirms that the design can detect subtle human motions if the following tolerances are maintained:

- **Phase Measurement Accuracy:** The system must maintain a phase resolution better than 0.1 radians.
- **Positional Tolerance:** The subject should ideally remain within a specified range from the center of the Fresnel zone to ensure maximal sensitivity.
- **Noise and Interference Control:** The environment must be managed to minimize extraneous reflections and electronic noise that could obscure these subtle phase changes.

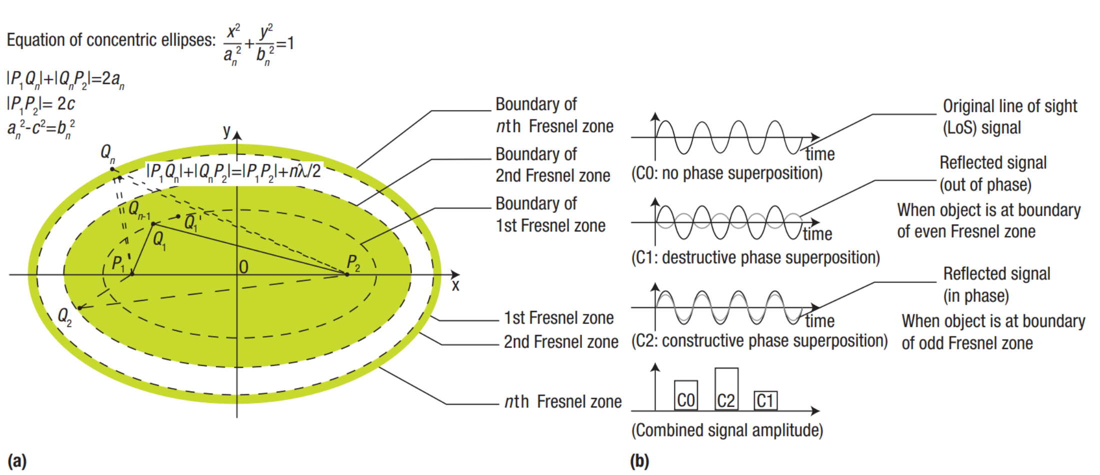

Figure 10: The Fresnel model.

3 Cost and Schedule

3.1 Cost Analysis

Table 6: Project Cost Breakdown

Category	Parts	Price (RMB)
Device	Lenovo V310-15	900
Microprocessor	PCB	200
Physical Model	Intel Ax200*2	115
	EDUP external antenna*2	108
	Aodeimao IPEX converter*4	24
	Chest model*2	60
	LED*6	20
	Counter*2	10
	Acrylic plates*5	50
	Stainless steel 304 damped hinges*12	28
Power Supply	3.3V/12V DC Power Supply	100
Labor	4 people * 80 hours * 75 RMB/hour	24000
Total	**25615**	

3.2 Schedule

Table 7: Schedule

Date	Yukai Han	Qiyang Wu	Xin Chen	Xuanqi Wang
4/18	Design appropriate surroundings for whole testing system	CSI extraction subsystem requirement analysis and hardware selection confirmation	Develop and refine scripts for circular buffering, phase correction, and filtering	Construct the power supply subsystem and design PCB
4/25	Construct surroundings using acrylic plates and hinges and test the strength	Debug and optimize the time domain filters and digital IF channel filters		Construct the PCB and LED
5/2	Fix chest models with LED, counters and acrylic plates	Complete software integration and tuning of CSI extraction subsystems	Debug and optimize the data processing pipeline	Help design circuits from signal output to LED display
5/9	Clean up all the items and lines of the system	Complete subsystem robustness test and anti-jamming capability verification		Further testing of the overall display system
5/16	Optimize the experimental equipment based on experimental results	Help design circuits from signal output to LED display	Integrate visual signal output with LED display	Improve the robustness of the display subsystem and debug under different scenarios
5/23	Prepare final testing demo	Prepare final demo and design testing cases	Prepare final demo	Prepare final demo and debug

4 Ethics and Safety

4.1 Ethics

Our project will strictly follow ethical standards by prioritizing public safety, privacy protection, and responsible technology use. Since we use WiFi signals to detect physiological activities, it inherently touches upon user privacy. We therefore ensure that no personally identifiable information is collected, and that all data remains anonymous to protect users' privacy. In accordance with the ACM Code of Ethics, we are committed to protecting the privacy and dignity of all individuals whose data may be used [6].

Furthermore, given the potential for misuse in tracking or surveillance, we design our system to prevent unauthorized exploitation. We don't store or display any data linked to an individual's identity. All data is processed locally and only for the purpose of modulating LED indicators for demonstration. Consistent with the IEEE Code of Ethics, we seek to avoid harm and uphold the public welfare through honest disclosures and responsible engineering practices [7].

To reinforce these commitments, every participant in our tests provides informed consent prior to data collection. The temporary data processing is clearly stated in a consent form. During any public display, a clear disclaimer will accompany our system to ensure it is not mistaken as a medical product. These precautions help uphold ethical transparency and prevent any misleading representation of the system's capabilities.

4.2 Safety

Our project strictly adheres to the safety standards set forth by the ECE 445 Safety Guidelines from the University of Illinois [8]. The system operates entirely at low voltage—3.3V and 12V DC—and does not involve any risky power levels, high temperatures, or moving mechanical parts. However, due to the presence of electronic circuitry, PCBs, and soldered components, we have implemented detailed precautions to ensure the safety of both users and developers.

All circuits are designed with current-limiting resistors and fuses to prevent overcurrent damage. During construction and testing, all exposed electrical connections are insulated including the use of ESD-safe mats and wrist straps when handling PCBs. Soldering is conducted in well-ventilated environments using heat-resistant tools as recommended by the course's safety documentation [8].

Prior to each lab session or demonstration, a safety checklist is reviewed to ensure stable power supply, secure wiring, and minimal electromagnetic interference in the testing environment. In accordance with ECE 445 protocol, we follow a two-person rule during high-risk activities such as circuit debugging or hardware testing. A formal safety manual will be presented at the final demo, summarizing all relevant precautions and emergency procedures, thereby demonstrating full compliance with the university's safety standards [8].

References

[1] Y. Zeng, D. Wu, J. Xiong, E. Yi, R. Gao, and D. Zhang, "Farsense: Pushing the range limit of wifi-based respiration sensing with csi ratio of two antennas," *Proceedings of the ACM on Interactive, Mobile, Wearable and Ubiquitous Technologies*, vol. 3, no. 3, pp. 1–26, 2019.

[2] A. Tzur, O. Amrani, and A. Wool, "Direction finding of rogue wi-fi access points using an off-the-shelf mimo–ofdm receiver," *Physical Communication*, vol. 17, pp. 149–164, 2015.

[3] E. Yi, F. Zhang, J. Xiong, K. Niu, Z. Yao, and D. Zhang, "Enabling wifi sensing on new-generation wifi cards," *Proceedings of the ACM on Interactive, Mobile, Wearable and Ubiquitous Technologies*, vol. 7, no. 4, pp. 1–26, 2024.

[4] X. Liang, H. H. Yang, K. Guo, and T. Q. Quek, "Enabling respiration sensing via commodity wifi 6e devices," in *GLOBECOM 2024-2024 IEEE Global Communications Conference*, IEEE, 2024, pp. 4382–4387.

[5] D. Zhang, H. Wang, and D. Wu, "Toward centimeter-scale human activity sensing with wi-fi signals," *Computer*, vol. 50, no. 1, pp. 48–57, 2017.

[6] Association for Computing Machinery. "ACM Code of Ethics and Professional Conduct." (2018), [Online]. Available: https://www.acm.org/code-of-ethics (visited on 04/13/2025).

[7] IEEE. "Ieee code of ethics." (2016), [Online]. Available: https://www.ieee.org/about/corporate/governance/p7-8.html (visited on 04/13/2025).

[8] University of lllinois at Urbana-champaign. "ECE 445 Safety Guidelines." (n.d), [Online]. Available: https://courses.grainger.illinois.edu/ece445zjui/guidelines/safety.asp (visited on 04/13/2025).